

Physics Methods for the Simulation of Photoionisation

Tullio Basaglia, Matej Batič, Min Cheol Han, Gabriela Hoff, Chan Hyeong Kim, Han Sung Kim, Maria Grazia Pia and Paolo Saracco

Abstract—Several physics methods for the simulation of the photoelectric effect are quantitatively evaluated with respect to a large collection of experimental data retrieved from the literature. They include theoretical and empirical calculations of total and partial cross sections, and calculations of the photoelectron angular distribution. Some of these models are currently implemented in general purpose Monte Carlo systems; some have been implemented and evaluated for possible use in Monte Carlo particle transport for the first time in this study.

I. INTRODUCTION

PHOTOIONIZATION is important in various experimental domains, such as material analysis applications, astrophysics, photon science and bio-medical physics. As one of the interactions photons undergo in matter, it is relevant in experimental methods concerned with the energy deposition resulting from photons as primary or secondary particles. Apart from elastic scattering at very low energies, photoionization is the dominant photon interaction in the low energy régime: as an example, below approximately 100 keV for target materials of atomic number around 30, and below approximately 700 keV for heavy target materials of atomic number close to 90. Photoionization is also experimentally relevant for the secondary atomic processes that it induces, X-ray fluorescence and Auger electron emission, which are play a relevant role in many physics research contexts and technological applications. Extensive reviews, that cover both the theoretical and experimental aspects of this process, can be found in the literature, for instance in [1]–[7] (this list of references is not intended to be exhaustive).

This paper is concerned with modeling the physics of photoionization under a pragmatic perspective: the simulation of this process in general purpose Monte Carlo codes for particle transport.

Calculations for the simulation of the photoelectric effect are implemented in all general purpose Monte Carlo systems, nevertheless a comprehensive, quantitative appraisal of their

validity is not yet documented in the literature. Assessments reported in the literature usually concern comparisons of cross sections with NIST reference values, such as [8], or involve complex observables resulting from many physics processes in the full simulation of an experimental set-up, such as [9]. In this respect, it is worthwhile to note that the validation of simulation models implies their comparison with experimental measurements [10]: comparisons with tabulations of theoretical calculations or analytical parameterizations, such as those that are reported in [11] as validation of Geant4 [12], [13] photon interaction cross sections, do not constitute a validation of the simulation software. Some relatively recent theoretical calculations and empirical analytical formulations documented in the literature have not been yet exploited in large scale Monte Carlo codes, nor have been comparatively evaluated in terms of accuracy and computational requirements with respect to currently used simulation methods.

The accuracy of simulation methods is quantified through statistical comparison with a wide collection of experimental data retrieved from the literature. These results provide guidance for the selection of physics models in simulation applications in response to the requirements of physics accuracy and computational speed pertinent to different experimental scenarios.

Special emphasis is devoted to the validation and possible improvement of photoionization simulation in Geant4; nevertheless, the results documented in this paper provide information relevant to other Monte Carlo systems as well.

The simulation of the atomic relaxation following the ionization of an atom has been treated in previous publications [14]–[17], therefore it is not included in the scope of this paper.

II. PHYSICS OVERVIEW

Photoionization has been the object of theoretical and experimental interest for several decades; only a brief overview is included here to facilitate the comprehension of the software features and the simulation validation results documented in this paper.

In the photoelectric effect a photon disappears and an electron is ejected from an atom. The energy of the photoelectron corresponds to the difference between the energy of the absorbed photon and the energy binding the electron to the atom.

The study reported here focuses on the evaluation and validation of basic physics features relevant to the simulation of the photoelectric effect: atomic cross sections and photoelectron angular distributions.

Manuscript received 15 November 2013.

This work has been partly funded by CNPq BEX6460/10-0 grant, Brazil.

T. Basaglia is with CERN, CH-1211, Geneva, Switzerland (e-mail: Tullio.Basaglia@cern.ch).

M. Batič was with INFN Sezione di Genova, Genova, Italy (e-mail: Batic.Matej@gmail.com); he is now with Sinergise, 1000 Ljubljana, Slovenia.

M. C. Han, C. H. Kim and H. S. Kim are with the Department of Nuclear Engineering, Hanyang University, Seoul 133-791, Korea (e-mail: mchan@hanyang.ac.kr, chkim@hanyang.ac.kr, hsungman@naver.com).

G. Hoff is with Pontificia Universidade Católica do Rio Grande do Sul, Brazil (e-mail: ghoff.gesic@gmail.com).

M. G. Pia and P. Saracco are with INFN Sezione di Genova, Via Dodecaneso 33, I-16146 Genova, Italy (phone: +39 010 3536328, fax: +39 010 313358, e-mail: MariaGrazia.Pia@ge.infn.it, Paolo.Saracco@ge.infn.it).

A. Total and partial cross sections

The photoelectric cross section as a function of energy exhibits a characteristic sawtooth behavior corresponding to absorption edges, as the binding energy of each electron subshell is attained and corresponding photoionization is allowed to occur.

Early theoretical calculations of photoionization cross sections were limited to the K shell; they are typified by the papers of Pratt [18], providing the asymptotic behavior for arbitrarily high energies, and Pratt et al. [19], reporting calculations in the energy range between 200 keV and 2 MeV. Only at a later stage more extensive calculations became available: Rakavy and Ron [20] calculated cross sections for all subshells of five elements over the energy range 1 keV to 2 MeV, Schmickley and Pratt [21] reported cross sections for K to M shells for three elements from 412 to 1332 keV.

Scofield's non-relativistic calculations [22] in a Hartree-Slater framework represented a major advancement in the field, as they covered systematically all subshells over the whole periodic table of the elements. More recent calculations were performed by Chantler [23], [24] in a self-consistent relativistic Dirac-Hartree-Fock framework.

Various empirical formulations of photoionization cross sections are reported in the literature, such as in [25]–[27]. They derive from fits to experimental data, parameterizations of theoretical calculations and semi-empirical methods involving both measured data and theoretical considerations.

Computational performance imposes constraints on the complexity of physics calculations to be performed in the course of simulation: hence the analysis in this paper is limited to theoretical cross sections for which tabulations of pre-calculated values are available and to empirical models that are expressed by means of simple analytical formulations. To be relevant for general purpose Monte Carlo systems, tabulated data should cover the whole periodic table of elements and an extended energy range.

The photoelectric cross section compilations considered in this study are summarized in Table I.

TABLE I
COMPILATIONS OF PHOTOIONIZATION CROSS SECTIONS

Compilation	Energy range		Z range		Shell
Biggs and Lighthill [26]	10 eV	100 GeV	1	100	
Brennan and Cowan [34]	30 eV	700 keV	3	92	
Chantler [23], [24]	10 eV	433 keV	1	92	K
Ebel [27]	1 keV	300 keV	1	92	all
Elam [35]	100 eV	1 MeV	1	98	
EPDL97 [36]	10 eV	100 GeV	1	100	all
Henke [37], [38]	10 eV	30 keV	1	92	
McMaster [39], [40]	1 keV	700 keV	1	94	
PHOTX [41]	1 keV	100 MeV	1	100	
RTAB [42]	10 eV	30 keV	1	99	all
Scofield [22]	1 keV	1.5 MeV	1	100	all
Storm and Israel [43]	1 keV	100 MeV	1	100	
Veigele [44]	100 eV	1 MeV	1	94	
XCOM [45]	1 keV	500 keV	1	100	

B. Angular distribution

Fischers non-relativistic theory [28] was derived for use in the low energy region. The first relativistic treatment of

the photoelectric effect was given by Sauter [29], [30], who calculated the K-shell cross section in the Born approximation; it is valid to the lowest order in $Z\alpha/\beta$ (where Z is the atomic number of the target, α is the fine structure constant and β is v/c). Gavrilu [31] and Nagel [32] extended Sauter's results to the next order in $Z\alpha/\beta$. Further calculations by Gavrilu are available for the L shel [33].

III. PHOTOIONIZATION IN MONTE CARLO CODES

General purpose Monte Carlo codes consider single photon interactions with isolated atoms in their ground state; they neglect interactions with ions and excited states, and multiple ionizations. Photon interactions are treated regardless of the environment of the target medium: this assumption neglects solid state effects and other features related to the molecular structure of the medium.

The original version of EGS4 [46] calculated photoelectric total cross sections based on Storm and Israel's tables [43] and generated the photoelectron with the same direction as the incident photon. Later evolutions introduced the use of PHOTX [41] cross sections [47] and the generation of the photoelectron angular distribution [48] based on Sauter's theory [29]. These features are currently implemented in EGS5 [49]. EGSnrc [50] provides the option of calculating total photoelectric cross sections based on Storm and Israel's tables as originally in EGS4 or on a fit to XCOM [45] cross sections, while it uses subshell cross sections based on EPDL [36]. It samples the photoelectron angular distribution according to the method described in [48] based on Sauter's theory.

ETRAN [51] uses Scofield's 1973 [22] cross sections for energies from 1 keV to 1.5 MeV and extends them to higher energies by exploiting Hubbell's method [25] to connect the values at 1.5 MeV to the asymptotic high energy limit calculated by Pratt [18]. It samples the direction of the photoelectron from Fischer's [28] distribution for electron energies below 50 keV and from the Sauter [29] distribution for higher energies.

FLUKA [52], [53] calculates photoelectric cross sections based on EPDL97 and samples the photoelectron direction according to Sauter's theory [29].

ITS [54] calculates photoelectric cross sections based on Scofield's 1973 non-renormalized values. The angle of the photoelectron with respect to the parent photon is described by Fischer's distribution [28] at lower energies and by Sauter's [29] formula at higher energies.

MCNP5 [55] and MCNPX [56] provide different options of data libraries for the calculation of photoelectric cross sections: two version of EPDL (EPDL97 [36] and EPDL89 [57]), and ENDF/B-IV [58] data complemented by Storm and Israel's tables [43] for atomic numbers greater than 83.

In the first version of Penelope including photon transport [59] photoelectric cross sections were interpolated from XCOM; in more recent versions [60], [61] they are interpolated from EPDL97 tabulations. The photoelectron angular distribution is sampled from Sauter's differential cross section for the K shell [29].

GEANT 3 [62] calculated total photoionization cross sections based on Biggs and Lighthill's [26] parameterizations;

the probability of ionization of the K shell and L subshells was estimated by parameterizations of the jump ratios deriving from Veigele's [44] tables. The angular distribution of the photoelectron was sampled for the K shell and for the L_1 , L_2 and L_3 subshells based on Sauter's [29], [30] and Gavrila's [31], [33] calculations.

The Geant4 toolkit encompasses various implementations of the photoelectric effect. The overview summarized here concerns the latest version at the time of the 2013 IEEE Nuclear science Symposium: Geant4 9.6, complemented by two correction patches.

The model implemented in Geant4 "standard" electromagnetic package [63] (also known as "Sandia Table") calculates cross sections based on the analytical formula of Biggs and Lighthill, but it reports using modified coefficients deriving from a fit to experimental data; nevertheless the reference cited in Geant4 9.6 Physics Reference Manual as the source of these modifications does not appear to be consistent. Presumably, the modifications derive from [64], which reports fits to experimental data concerning noble gases, hydrogen, carbon, fluorine, oxygen and silicon. The energy of the emitted photoelectron is determined as the difference between the energy of the interacting photon and the binding energy of the ionized shell defined in the *G4AtomicShells* class [17], and the photoelectron angle is calculated according to the Sauter-Gavrila distribution for K shell [29], [31].

Geant4 low energy electromagnetic package [65], [66] encompasses two implementations of the photoelectric effect, one identified as "Livermore" [67] and one reengineered from the 2008 version of the Penelope code [60]: both models calculate total and partial cross sections based on EPDL97. The so-called "Livermore" model provides three options of computing the angular distribution of the emitted photoelectron: in the same direction as the incident photon, based on Gavrila's distribution of the polar angle [31] for the K shell and the L_1 subshell, and based on a double differential cross section derived from Gavrila's [31], [33] calculations, which can also handle polarized photons.

In addition, the Geant4 toolkit encompasses two models for the simulation of the photoelectric effect concerning polarized photons: one for circularly polarised photons in the "polarisation" package and one in the low energy electromagnetic package, identified as "Livermore polarised". Polarized photons are not considered in this study.

IV. STRATEGY OF THIS STUDY

An extensive set of simulation models, which are representative of the variety of theoretical and empirical approaches documented in the literature, have been evaluated to identify the state-of-the-art of modeling photoionization in the context of Monte Carlo particle transport.

The models for the simulation of photoionization evaluated in this paper concern total and partial cross sections: in particle transport, the former are relevant to determine the occurrence of the photoionization process, while the latter determine the creation of a vacancy in a specific shell.

In addition, formulations of the photoelectron angular distribution have been evaluated.

All the models subject to study have been implemented in a consistent software design, compatible with the Geant4 toolkit, which minimizes external dependencies to ensure the unbiased appraisal of their intrinsic capabilities.

A wide set of experimental data has been collected from the literature for this study; simulation models are validated through comparison with these measurements. The compatibility with experiment for each model, and the differences in compatibility with experiment across the various models, are quantified by means of statistical methods.

A. Software environment

All the physics models evaluated in this paper have been implemented in the same software environment, which is compatible with Geant4; computational features specific to the original physics algorithms have been preserved as much as possible. The uniform software configuration ensures an unbiased appraisal of the intrinsic characteristics of the various physics models. The correctness of implementation has been verified prior to the validation process to ensure that the software reproduces the physical features of each model consistently.

The software adopts a policy-based class design [68]; this technique was first introduced in a general-purpose Monte Carlo system in [69].

Two policies have been defined for the simulation of photoionization, corresponding to the calculation of total cross section and to the generation of the final state; they conform to the prototype design described in [70], [71]. A photoionization process, derived from the *G4VDiscreteProcess* class of Geant4 kernel, acts as a host class for these policy classes. All the simulation models implemented according to this policy-based class design are compatible for use with Geant4, since Geant4 tracking handles all discrete processes polymorphically through the *G4VDiscreteProcess* base class interface.

A single policy class calculates total cross sections for all the physics models that exploit tabulations; alternative tabulations, corresponding to different physics models, are managed through the file system. Specific policy classes implement the analytical calculations of Biggs and Lighthill (accounting for the modifications adopted in Geant4 "standard" electromagnetic package) and of Ebel.

Three photoelectron angular distribution models have been implemented: they correspond to the Sauter-Gavrila formulation as in Geant4 "standard" electromagnetic package, to the Sauter-Gavrila formulation as in the *G4PhotoElectricAngularGeneratorPolarized* class of Geant4 low energy electromagnetic package, and to a formulation based on corrected GEANT 3 code.

The software design adopted in this study ensures greater flexibility than the design currently adopted in Geant4 electromagnetic package, since it allows independent modeling and test of the various physics features of photoionization.

B. Experimental data

Experimental data for the validation of the simulation models were collected from a survey of the literature. Only cross

sections that were directly measured were considered in the validation process; semi-empirical evaluations, derived from experimental measurements from which theoretical scattering cross section were subtracted to extract photoelectric cross sections, were not considered.

The sample of experimental cross sections consists of more than 5000 measurements: approximately 3700 total cross sections and 1400 shell cross sections, respectively. Due to the limited page allocation typical of conference proceedings, the extensive bibliographical references of the experimental data sample will be included in a forthcoming publication to be submitted to IEEE Transactions on Nuclear Science.

C. Data analysis method

The evaluation of the simulation models performed in this study has two objectives: to validate them quantitatively, and to compare their relative capabilities.

The scope of the software validation process is defined according to the guidelines of the pertinent IEEE Standard [72]. For the problem domain considered in this paper, the validation process provides evidence that the software models photoionization consistent with experiment.

The analysis of cross sections is articulated over two stages: the first one estimates the compatibility between the values calculated by each simulation model and experimental data, while the second exploits the results of the first stage to determine whether the various models exhibit any significant differences in their compatibility with experiment.

The first stage encompasses a number of test cases, each one corresponding to a photon energy and target element for which experimental data are available. For each test case, cross sections calculated by the software are compared with experimental measurements by means of goodness-of-fit tests; the null hypothesis is defined as the equivalence of the simulated and experimental data distributions subject to comparison.

The goodness-of-fit analysis is based on the χ^2 test [73] and utilizes the Statistical Toolkit [74], [75]. The level of significance is 0.01. The “efficiency” of a physics model is defined as the fraction of test cases in which the χ^2 test does not reject the null hypothesis at 0.01 level of significance.

The second stage of the statistical analysis quantifies the differences of the simulation models in compatibility with experiment. It consists of a categorical analysis based on contingency tables, which derive from the results of the χ^2 test: the outcome of this test is classified as “fail” or “pass”, according respectively to whether the hypothesis of compatibility of experimental and calculated data is rejected or not.

The null hypothesis in the analysis of a contingency table assumes the equivalent compatibility with experiment of the models it compares. Contingency tables are analyzed with Fisher’s exact test [76], Barnard’s exact test [77] and Pearson’s χ^2 test [78] (the last one when appropriate). The use of different tests mitigates the risk of introducing systematic effects, which could be due to the peculiar mathematical properties of a single test.

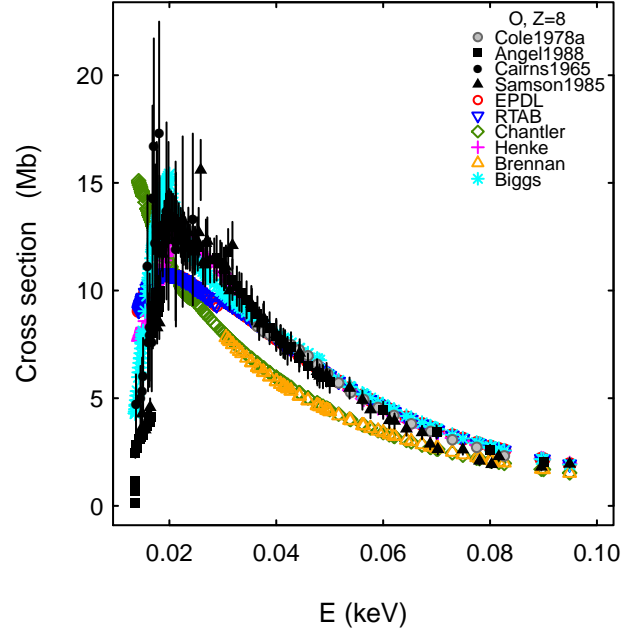


Fig. 1. Total photoionization cross section for Z=8 as a function of photon energy.

The significance level for the rejection of the null hypothesis in the analysis of contingency tables is 0.05, unless differently specified.

Due to the scarcity of experimental data and the unclear systematics in the measurements, a statistical analysis of photoelectron angular distribution would not be meaningful. For this observable the comparison with experimental data is limited to qualitative appraisal.

V. RESULTS

Only a brief summary of the results of the validation process is reported here; the full set of results will be documented in detail in a forthcoming journal publication.

A. Total Cross Sections

Figs. 1 and 2 illustrate two examples of calculated and experimental total cross sections.

The “efficiency” of the various total cross section calculation methods is documented in Fig. 3: most methods exhibit similar compatibility with experiment for photon energies greater than 250 eV, while degraded accuracy is observed at lower energies. Two cross section calculation methods exhibit lower compatibility with experiment in Fig. 3; this qualitative observation is confirmed quantitatively by the results of the analysis of contingency tables reported in Table II, where their compatibility with experimental data is compared with that of EPDL: for both models all the tests applied to the associated contingency tables show that the hypothesis of equivalent performance with respect to EPDL is rejected with 0.05 significance.

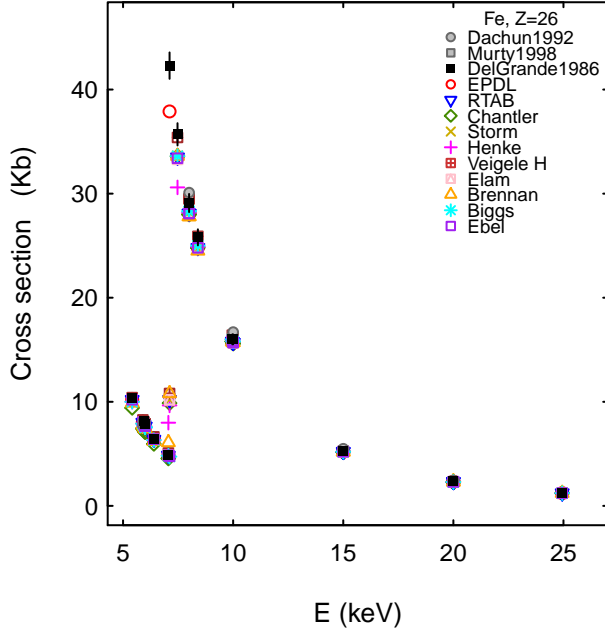


Fig. 2. Total photoionization cross section for $Z=26$ as a function of photon energy.

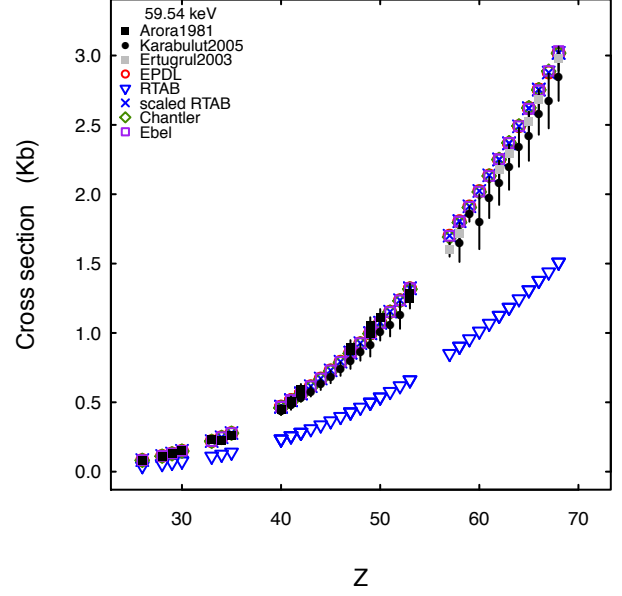


Fig. 4. Cross section for photoionization of the K shell at 59.54 keV as a function of atomic number.

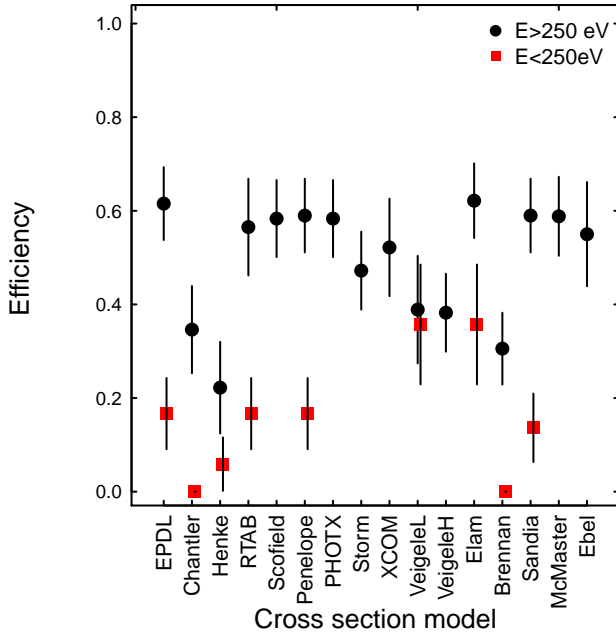


Fig. 3. Efficiency of the total cross section calculation methods subject to test.

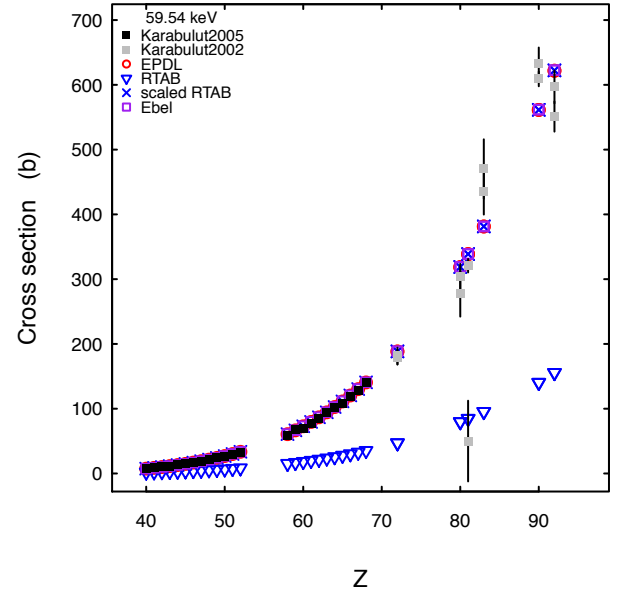


Fig. 5. Cross section for photoionization of the L_3 subshell at 59.54 keV as a function of atomic number.

TABLE II

P-VALUES RESULTING FROM CONTINGENCY TABLES COMPARING THE COMPATIBILITY WITH EXPERIMENT OF CHANTLER AND EPDL TOTAL CROSS SECTION CALCULATIONS, AND OF BRENNAN AND COWAN AND EPDL CALCULATIONS.

Test	Chantler - EPDL	Brennan and Cowan - EPDL
Fisher	0.044	0.011
χ^2	0.033	0.007
Barnard	0.035	0.007

B. Shell Ionization Cross Sections

Figs. 4 to 7 illustrate some examples of calculated and experimental cross sections for inner and outer shell photoionization.

A systematic discrepancy of RTAB shell cross sections with respect to experimental data is observed, which hints to a missing multiplicative factor in the tabulated values. When RTAB cross sections are scaled by the presumed missing factor, they exhibit compatibility with experiment comparable to other calculation methods.

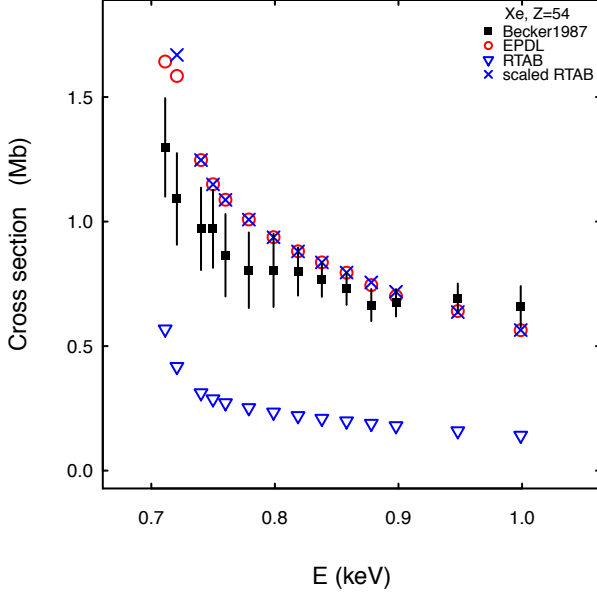


Fig. 6. Cross section for photoionization of the M_4 subshell of xenon as a function of energy.

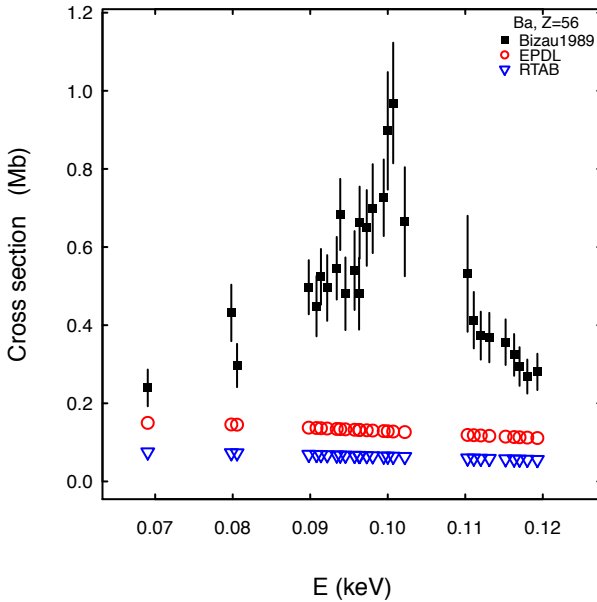


Fig. 7. Cross section for photoionization of the O_1 subshell of barium as a function of energy.

The p-values resulting from the χ^2 test listed in Table III show that, once RTAB values are rescaled, all calculation methods determine K and L shell cross sections that are compatible with experimental data with 0.05 significance, with the exception of Ebel's parameterized model. The cross sections for outer shells appear incompatible with experiment; nevertheless one should take into account that the experimental data samples available for the validation of outer shells are small, and often the data for a given test case originate from a single experimental source, which could be affected by

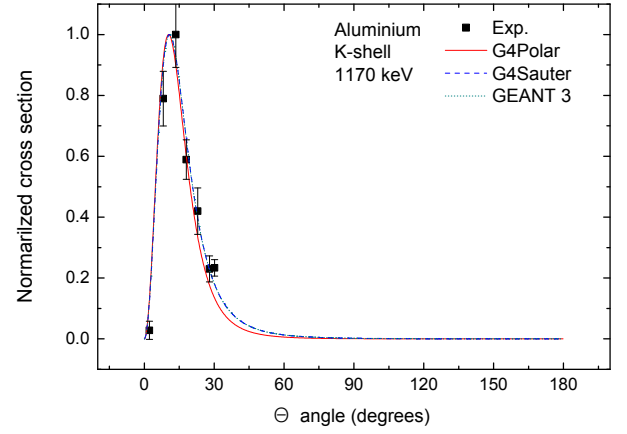


Fig. 8. Photoelectron angular distribution for aluminium, K shell, at 1.17 MeV.

systematic effects.

TABLE III
P-VALUES OF THE χ^2 TEST FOR COMPATIBILITY OF SHELL CROSS SECTIONS WITH EXPERIMENTAL DATA

shell	EPDL	Chantler	RTAB	RTAB (scaled)	Ebel
K	0.209	0.350	< 0.001	0.315	< 0.001
L₁	0.075		< 0.001	0.069	0.964
L₂	0.339		< 0.001	0.299	0.154
L₃	1		< 0.001	1	1
M₁	< 0.001		< 0.001	< 0.001	
M₄	0.031		< 0.001	< 0.001	
M₅	< 0.001		< 0.001	< 0.001	
N₁	< 0.001		< 0.001	< 0.001	
N₆	< 0.001		< 0.001	< 0.001	< 0.001
N₇	< 0.001		< 0.001	< 0.001	< 0.001
O₁	< 0.001		< 0.001	< 0.001	< 0.001
O₂	< 0.001		< 0.001	< 0.001	< 0.001
O₃	< 0.001		< 0.001	< 0.001	< 0.001
P₁	< 0.001		< 0.001	< 0.001	< 0.001

C. Photoelectron Angular Distribution

Two examples of angular distributions are shown in Figs. 8 and 9. The limited experimental data sample does not allow a meaningful statistical analysis.

VI. CONCLUSION

An extensive set of models for the simulation of photoionization has been quantitatively evaluated regarding their accuracy at reproducing experimental measurements.

All total cross section calculation methods are equivalent in terms of compatibility with experimental data, with the exception of those calculated by Chantler and by Brennan and Cowan. The fraction of test cases that are compatible with experiment drops at energies below 250 eV.

Inner shell cross section calculations are compatible with experimental data, with the exception of Ebel's parameterization for the K shell. Outer shell photoionization cross sections are incompatible with experimental data; nevertheless the limited data sample hints not to draw any hasty conclusions about the accuracy of the examined models.

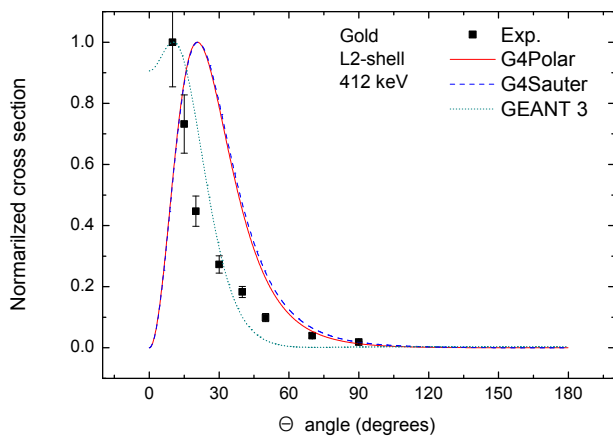


Fig. 9. Photoelectron angular distribution for gold, L_2 subshell, at 412 keV.

Due to the scarce availability of experimental data and possible systematic effects in the reported measurements, only a qualitative appraisal of photoelectron angular distribution models is possible. All Geant4 angular distribution models exhibit a similar behavior; the corrected GEANT 3 model appears in some cases different from the others and qualitatively competitive.

The full set of results will be documented in a forthcoming journal publication.

ACKNOWLEDGMENT

The CERN Library has provided helpful assistance and essential reference material for this study.

REFERENCES

- [1] R. H. Pratt, A. Ron, and H. K. Tseng, "Atomic photoeffect above 10 keV", *Rev. Mod. Phys.*, vol. 45, 273-325, 1973.
- [2] R. H. Pratt, A. Ron, and H. K. Tseng, "Erratum: Atomic photoeffect above 10 keV", *Rev. Mod. Phys.*, vol. 45, 663-664, 1973.
- [3] J. A. R. Samson, "Photoionization of atoms and molecules", *Phys. Rep.*, vol. 28, no. 4, pp. 303-354, 1976.
- [4] H. P. Kelly, "Review of our present understanding of the photoionization process for atoms", *AIP Conf. Proc.*, vol. 215, pp. 292-311, 1990.
- [5] A. F. Starace, "Photoionization of atoms", in *Atomic, Molecular and Optical Physics Handbook*, Springer, Berlin, pp. 379-390, 2006.
- [6] M. Y. Amusia, "Atomic Photoeffect", Plenum, New York, 1990.
- [7] J. Berkowitz, "Atomic and Molecular Photoabsorption", Academic Press, London, 2002.
- [8] K. Amako et al., "Comparison of Geant4 electromagnetic physics models against the NIST reference data", *IEEE Trans. Nucl. Sci.*, vol. 52, no. 4, pp. 910-918, 2005.
- [9] U. Chica, M. Anguiano, and A. M. Lallena, "Benchmark of PENELOPE for low and medium energy X-rays", *Phys. Med.*, vol. 25, no. 2, pp. 5157, 2009.
- [10] T. G. Trucano, L. P. Swiler, T. Igusa, W. L. Oberkampf, and M. Pilch, "Calibration, validation, and sensitivity analysis: Whats what", *Reliab. Eng. Syst. Safety*, vol. 91, no. 10-11, pp. 1331-1357, 2006.
- [11] G. A. P. Cirrone, G. Cuttone, F. Di Rosa, L. Pandola, F. Romano, and Q. Zhang, "Validation of the Geant4 electromagnetic photon cross-sections for elements and compounds", *Nucl. Instr. Meth. A*, vol. 618, pp. 315-322, 2010.
- [12] S. Agostinelli et al., "Geant4 - a simulation toolkit" *Nucl. Instrum. Meth. A*, vol. 506, no. 3, pp. 250-303, 2003.
- [13] J. Allison et al., "Geant4 Developments and Applications" *IEEE Trans. Nucl. Sci.*, vol. 53, no. 1, pp. 270-278, 2006.

- [14] S. Guatelli, A. Mantero, B. Mascialino, P. Nieminen, and M. G. Pia, "Geant4 Atomic Relaxation", *IEEE Trans. Nucl. Sci.*, vol. 54, no. 3, pp. 585-593, 2007.
- [15] S. Guatelli et al., "Validation of Geant4 Atomic Relaxation against the NIST Physical Reference Data", *IEEE Trans. Nucl. Sci.*, vol. 54, no. 3, pp. 594-603, 2007.
- [16] M. G. Pia, P. Saracco, and M. Sudhakar, "Validation of K and L Shell Radiative Transition Probability Calculations", *IEEE Trans. Nucl. Sci.*, vol. 56, no. 6, pp. 3650-3661, 2009.
- [17] M. G. Pia et al., "Evaluation of atomic electron binding energies for Monte Carlo particle transport", *IEEE Trans. Nucl. Sci.*, vol. 58, no. 6, pp. 3246-3268, 2011.
- [18] R. H. Pratt, "Atomic photoelectric effect at high energies", *Phys. Rev.*, vol. 117, pp. 1017-1028, 1960.
- [19] R. H. Pratt, "K-Shell Photoelectric Cross Sections from 200 keV to 2 MeV", *Phys. Rev.*, vol. 134, pp. A898-A915, 1964.
- [20] G. Rakavy and A. Ron, "Atomic Photoeffect in the Range $E_\gamma=1-2000$ keV", *Phys. Rev.*, vol. 159, pp. 50-56, 1960.
- [21] R. D. Schmickley and R. Pratt, "K-, L-, and M-shell atomic photoeffect for screened-potential models", *Phys. Rev.*, vol. 164, pp. 104-116, 1967.
- [22] J. H. Scofield, "Theoretical photoionization cross sections from 1 to 1500 keV", Report UCRL-51326, Lawrence Livermore Laboratory, 1973.
- [23] C. T. Chantler, "Theoretical form factor, attenuation and scattering tabulation for $Z=192$ from $E=110$ eV to $E=0.410$ MeV", *J. Phys. Chem. Ref. Data*, vol. 24, no. 1, pp. 71643, 1995.
- [24] C. T. Chantler, "Detailed tabulation of atomic form factors, photoelectric absorption and scattering cross section, and mass attenuation coefficients in the vicinity of absorption edges in the soft X-ray ($Z=30-36$, $Z=60-89$, $E=0.1$ keV-10 keV), addressing convergence issues of earlier work", *J. Phys. Chem. Ref. Data*, vol. 29, no. 4, pp. 597-1048, 2000.
- [25] J. H. Hubbell, "Photon Cross Sections, Attenuation Coefficients, and Energy Absorption Coefficients from 10 keV to 100 GeV", Report NSRDS-NBS 29, National Bureau of Standards, Washington, DC (USA), 1969.
- [26] F. Biggs and R. Lighthill, "Analytical Approximations for X-RayCrossSections III" Sandia National Laboratories Report SAND87-0070, Albuquerque, 1988.
- [27] H. Ebel, R. Svagera, M. F. Ebel, A. Shaltout, and J. H. Hubbell, "Numerical description of photoelectric absorption coefficients for fundamental parameter programs", *X-Ray Spectrom.*, vol. 32, no. 6, pp. 442451, 2003.
- [28] F. Fischer, "Beiträge zur Theorie der Absorption von Röntgenstrahlung", *Ann. Phys.*, vol. 400, no. 7, pp. 821-850, 1931.
- [29] F. Sauter, "Über den atomaren Photoeffekt in der K-Schale nach der relativistischen Wellenmechanik Diracs", *Ann. Phys.*, vol. 403, no. 4, pp. 454-488, 1931.
- [30] F. Sauter, "Über den atomaren Photoeffekt bei großer Härte der anregenden Strahlung", *Ann. Phys.*, vol. 401, no. 2, pp. 217-248, 1931.
- [31] M. Gavril, "Relativistic k-shell photoeffect", *Phys. Rev.*, vol. 113, pp. 514-536, 1959.
- [32] B. Nagel, "Angular distribution and polarization of K-shell photoelectrons in the high energy limit", *Ark. Fys.*, vol. 24, pp. 151-159, 1963.
- [33] M. Gavril, "Relativistic l-shell photoeffect", *Phys. Rev.*, vol. 124, pp. 1132-1141, 1961.
- [34] S. Brennan and P. L. Cowan, "A suite of programs for calculating xray absorption, reflection, and diffraction performance for a variety of materials at arbitrary wavelengths", *Rev. Sci. Instrum.*, vol. 63, pp. 850-853, 1992.
- [35] W. Elam, B. Ravel, and J. Sieber, "A new atomic database for X-ray spectroscopic calculations", *Radiat. Phys. Chem.*, vol. 63, pp. 121-128, 2002.
- [36] D. Cullen et al., "EPDL97, the Evaluated Photon Data Library", Lawrence Livermore National Laboratory Report UCRL-50400, Vol. 6, Rev. 5, 1997.
- [37] B. L. Henke, P. Lee, T. Tanaka, R. L. Shimabukuro, and B. Fujikawa, "Low-energy X-ray interaction coefficients: Photoabsorption, scattering, and reflection: $E=1002000$ eV $Z=194$ ", *Atom. Data Nucl. Data Tables*, vol. 27, pp. 1-144, 1982.
- [38] B. L. Henke, E. M. Gullikson, and J. C. Davis, "X-Ray Interactions: Photoabsorption, Scattering, Transmission, and Reflection at $E=50-30000$ eV, $Z=1-92$ ", *Atom. Data Nucl. Data Tables*, vol. 54, no. 2, pp. 181342, 1993.

- [39] W. H. McMaster, N. Kerr Del Grande, J. H. Mallet and J. H. Hubbell, "Compilation of X-ray cross sections", Section II Revision 1, Lawrence Livermore National Laboratory Report UCRL-50174, 1969.
- [40] A. Shaltout, H. Ebel, and R. Svagera, "Update of photoelectric absorption coefficients in the tables of McMaster", *X-Ray Spectrom.*, vol. 35, pp. 52-56, 2006.
- [41] D. K. Trubey, M. J. Berger, and J. H. Hubbell, "Photon cross sections for ENDF/B-VI", Oak Ridge National Lab. Report CONF-890408-4, 1989.
- [42] L. Kissel, "RTAB: the Rayleigh scattering database", *Radiat. Phys. Chem.*, vol. 59, pp. 185-200, 2000.
- [43] E. Storm and H. I. Israel, "Photon cross sections from 1 keV to 100 MeV for elements Z=1 to Z=100", *Atom. Data Nucl. Data Tables*, vol. 7, pp. 565-681, 1970.
- [44] W. M. J. Veigele, "Photon cross sections from 0.1 keV to 1 MeV for elements Z = 1 to Z= 94", *Atom. Data Nucl. Data Tables*, vol. 5, no. 1, pp. 51-111, 1973.
- [45] M. J. Berger et al., "XCOM: Photon Cross section Database (version 1.5)", National Institute of Standards and Technology, Gaithersburg, MD, 2010. [Online] Available: <http://physics.nist.gov/xcom>.
- [46] W. R. Nelson, H. Hirayama, and D. W. O. Rogers, "The EGS4 Code System", SLAC-265 Report, Stanford, CA, 1985.
- [47] Y. Sakamoto, "Photon cross section data PHOTX for PEGS4 code", in *Proc. Third EGS4 Users Meeting in Japan*, KEK Proceedings 93-15, pp. 7782, Japan, 1993.
- [48] A. F. Bielajew and D. W. O. Rogers, "Photoelectron angular distribution in the EGS4 code system", Report PIRS-0058, National Research Council of Canada, 1986.
- [49] H. Hirayama, Y. Namito, A. F. Bielajew, S. J. Wilderman, and W. R. Nelson, "The EGS5 Code System", SLAC-R-730 Report, Stanford, CA, 2006.
- [50] I. Kawrakow, E. Mainegra-Hing, D.W.O. Rogers, F. Tessier and B.R.B. Walters, "The EGSnrc Code System: Monte Carlo Simulation of Electron and Photon Transport NRCC PIRS-701, 5th printing, 2010.
- [51] S. M. Seltzer, "Electron-Photon Monte Carlo Calculations: The ETRAN Code", *Appl. Radiat. Isot.*, vol. 42, no. 10, pp. 917-941, 1991.
- [52] G. Battistoni et al., "The FLUKA code: description and benchmarking", *AIP Conf. Proc.*, vol. 896, pp. 31-49, 2007.
- [53] A. Ferrari et al., "Fluka: a multi-particle transport code", Report CERN-2005-010, INFN/TC-05/11, SLAC-R-773, Geneva, Oct. 2005.
- [54] B. C. Franke, R. P. Kensek and T. W. Laub, "ITS5 theory manual", rev. 1.2, Sandia Natl. Lab. Report SAND2004-4782, Albuquerque, 2004.
- [55] X-5 Monte Carlo Team, "MCNP – A General Monte Carlo N-Particle Transport Code, Version 5", Los Alamos National Laboratory Report LA-UR-03-1987, 2003, revised 2008.
- [56] D. B. Pelowitz et al., "MCNPX 2.7.E Extensions", Los Alamos National Laboratory Report LA-UR-11-01502, 2011.
- [57] D. E. Cullen et al., "Tables and Graphs of Photon Interaction Cross Sections from 10 eV to 100 GeV Derived from the LLNL Evaluated Photon Data Library (EPDL)", Lawrence Livermore National Laboratory Report UCRL-50400, Vol. 6, Rev. 4, 1989.
- [58] D. Garber Ed. , "ENDF/B Summary Documentation", BNL-17541, 1975.
- [59] J. Sempau, E. Acosta, J. Baro, J. M. Fernandez-Varea, and J. Salvat, "An algorithm for Monte Carlo simulation of coupled electron-photon transport", *Nucl. Instrum. Meth. B*, vol. 132, pp. 377-390, 1997.
- [60] F. Salvat, J.M. Fernandez-Varea, and J. Sempau, "Penelope - A code system for Monte Carlo simulation of electron and photon transport", Proc. Workshop NEA 6416, 2008.
- [61] F. Salvat, J.M. Fernandez-Varea, and J. Sempau, "Penelope-2011 - A code system for Monte Carlo simulation of electron and photon transport", Proc. Workshop NEA/NSC/DOC(2011)5, 2011.
- [62] "GEANT Detector Description and Simulation Tool", CERN Program Library Long Writeup W5013, 1995.
- [63] H. Burkhardt et al., "Geant4 Standard Electromagnetic Package", in *Proc. 2005 Conf. on Monte Carlo Method: Versatility Unbounded in a Dynamic Computing World*, Am. Nucl. Soc., USA, 2005.
- [64] V. M. Grishin, A. P. Kostin, S. K. Kotelnikov and D. G. Streblechenko, Parametrization of the photoabsorption cross section at low energies", *Bull. Lebedev Inst.*, no. 6, pp. 1-6, 1994.
- [65] S. Chauvie, G. Depaola, V. Ivanchenko, F. Longo, P. Nieminen and M. G. Pia, "Geant4 Low Energy Electromagnetic Physics", in *Proc. Computing in High Energy and Nuclear Physics*, Beijing, China, pp. 337-340, 2001.
- [66] S. Chauvie et al., "Geant4 Low Energy Electromagnetic Physics", in *2004 IEEE Nucl. Sci. Symp. Conf. Rec.*, pp. 1881-1885, 2004.
- [67] J. Apostolakis, S. Giani, M. Maire, P. Nieminen, M.G. Pia, L. Urban, "Geant4 low energy electromagnetic models for electrons and photons" *INFN/AE-99/18*, Frascati, 1999.
- [68] A. Alexandrescu, "Modern C++ Design", Ed.: Addison-Wesley, 2001.
- [69] S. Chauvie et al., "Geant4 physics processes for microdosimetry simulation: design foundation and implementation of the first set of models", *IEEE Trans. Nucl. Sci.*, vol. 54, no. 6, pp. 2619-2628, 2007.
- [70] M. Augelli et al., "Research in Geant4 electromagnetic physics design, and its effects on computational performance and quality assurance", in *2009 IEEE Nucl. Sci. Symp. Conf. Rec.*, pp. 177-180, 2009.
- [71] M. G. Pia et al., "Design and performance evaluations of generic programming techniques in a R&D prototype of Geant4 physics", *J. Phys.: Conf. Ser.*, vol. 219, pp. 042019, 2010.
- [72] IEEE Computer Society, "IEEE Standard for Software Verification and Validation", IEEE Std 1012-2004, Jun. 2005.
- [73] R. K. Bock and W. Krischer, "The Data Analysis BriefBook ", Ed. Springer, Berlin, 1998.
- [74] G. A. P. Cirrone et al., "A Goodness-of-Fit Statistical Toolkit", *IEEE Trans. Nucl. Sci.*, vol. 51, no. 5, pp. 2056-2063, 2004.
- [75] B. Mascialino, A. Pfeiffer, M. G. Pia, A. Ribon, and P. Viarengo, "New developments of the Goodness-of-Fit Statistical Toolkit", *IEEE Trans. Nucl. Sci.*, vol. 53, no. 6, pp. 3834-3841, 2006.
- [76] R. A. Fisher, "On the interpretation of χ^2 from contingency tables, and the calculation of P", *J. Royal Stat. Soc.*, vol. 85, no. 1, pp. 87-94, 1922.
- [77] G. A. Barnard, "Significance tests for 2 x 2 tables", *Biometrika*, vol. 34, pp. 123-138, 1947.
- [78] K. Pearson, "On the χ^2 test of Goodness of Fit", *Biometrika*, vol. 14, no. 1-2, pp. 186-191, 1922.